Polyhedron 76 (2014) 29–35

Contents lists available at ScienceDirect

Polyhedron

journal homepage: www.elsevier.com/locate/poly

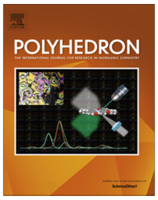

Octahedral Ni(II) and Cu(II) complexes with a new hexadentate $(NSN)_2$ donor ligand: Synthesis, characterization, X-ray structure and DFT calculations

Mahendra Sekhar Jana, Ajoy Kumar Pramanik, Tapan Kumar Mondal [*]

Inorganic Chemistry Section, Department of Chemistry, Jadavpur University, Kolkata 700032, India

ARTICLE INFO

Article history:
Received 8 November 2013
Accepted 23 March 2014
Available online 5 April 2014

Keywords:
Octahedral Ni(II) and Cu(II) complexes
Hexadentate arylazothioether ligand
X-ray structure
DFT and TDDFT calculations

ABSTRACT

Coupling of arylthioether diazonium salts with acetylacetone in NaOH medium produced the hexadentate ligand **HL**. This ligand can undergo keto-enol tautomerism in solution. It acts as a monoanionic hexadentate (N,S,N,N,S,N) chelator and forms 1:1 isostructural complexes, $[Ni(L)](ClO_4)$ (**1**) and $[Cu(L)](ClO_4)$ (**2**), with Ni(II) and Cu(II) respectively. The complexes have been characterized by spectral analysis. The pseudo octahedral geometries of the complexes are confirmed by single crystal X-ray diffraction studies. The X-ray and spectral characterizations confirmed the existence of the keto form of the ligand in the complexes. The electronic structures and spectral properties of the ligand and the complexes have been explained by DFT and TDDFT calculations.

1. Introduction

The coordination chemistry of N, S donor ligands has received a great deal of attention due to the stability, chemical and electrochemical activities, and biological relevance of the corresponding complexes [1–7]. Thiols and thioethers are ubiquitous donor functions in the active sites of many naturally occurring metalloenzymes. In the coordination sphere of redox active metal ions such as iron, cobalt, copper, etc., sulfur-ligands affect a high redox potential because the reduced metal center is a softer cation and therefore more efficiently coordinated by the soft sulfur donors [8,9].

Polydentate ligands with thioether moieties are often used for the synthesis of model complexes to mimic the spectroscopic and structural properties of the active sites of metalloproteins [10–13]. Complexes containing N, S donor ligands have biological relevance as several bioactive molecules contain similar donor environments [14–18]. The potential role played by nickel(II) and copper(II) ions, being present in the active sites of a large number of metalloproteins, have encouraged the design of new ligand frames having nitrogen–sulfur donor centres, characterization of nickel and copper complexes as models for providing a better understanding of biological systems and for assisting in the development of new homogeneous catalysts for selective catalytic reactions [19–24]. Moreover, the presence of nickel-sulfur and -nitrogen bonds at the active sites of several hydrogenases [25] and carbon monoxide dehydrogenases [26] has stimulated interest in nickel chemistry with mixed sulfur and nitrogen donor ligands [27].

The substitution of an aryl diazonium group at the active methylinic carbon of acetylacetone and the study of azo-hydrazone tautomerism have been reported elsewhere [28–30]. Herein, we have synthesized the new hexadentate N(pyridyl), S(thioether) and N(azo) donor ligand, **HL** by substituting both of the active methylene protons and eliminating an acetyl group in strongly alkaline medium. The structural characterization of the ligand has been carried out by ^1H NMR and mass spectroscopy, and elemental analysis. The octahedral Ni(II) and Cu(II) complexes with this ligand have been synthesized and characterized by different experimental techniques abetted with theoretical computations.

2. Experimental

2.1. Materials and methods

2-((Pyridine-2-yl)methylthio)benzenamine was prepared following the reported procedure [31]. 2-Aminothiophenol and 2-(chloromethyl)pyridine were purchased from Sigma Aldrich. All other chemicals and solvents were of reagent grade and used as received.

---

[*] Corresponding author. Tel.: +91 033 24146666x2453; fax: +91 033 24146584.
E-mail address: tkmondal@chemistry.jdvu.ac.in (T.K. Mondal).

http://dx.doi.org/10.1016/j.poly.2014.03.052
0277-5387/© 2014 Elsevier Ltd. All rights reserved.

Table 1
Crystal data and details of the structure determination for **1** and **2**.

Crystal data	**1**	**2**
Formula	$C_{27}H_{23}N_6NiOS_2$, ClO_4	$C_{27}H_{23}CuN_6OS_2$, ClO_4
Formula weight	669.79	674.62
Crystal system	triclinic	monoclinic
Space group	$P\bar{1}1$	$P21/c$
a (Å)	9.867(5)	9.708(5)
b (Å)	10.955(5)	27.984(5)
c (Å)	14.746(5)	11.326(5)
α (°)	110.041(5)	90
β (°)	95.807(5)	108.210(5)
γ (°)	106.865(5)	90
V (Å^3)	1396.9(11)	2923(2)
Z	2	4
ρ_{calc} (g cm^{-3})	1.592	1.533
μ (mm^{-1})	0.990	1.030
$F(000)$	688	1380
Data collection		
T (K)	293(2)	293(2)
λ (Å)	0.71073	0.71073
$\theta_{min-max}$ (°)	1.51–25.08	2.03–27.16
hkl range	−10 to 11, −13 to 13, −17 to 17	−12 to 12, −35 to 35, −14 to 14
Total, Unique Data, R_{int}	19751, 4859, 0.0284	47254, 6460, 0.1036
Observed data [$I > 2\sigma(I)$]	3649	3121
Refinement		
N_{ref}, N_{par}	4859, 379	6460, 379
R, wR_2 ($I > 2\sigma(I)$)	0.0426, 0.1015	0.0604, 0.1259
R, wR_2 (all data)	0.0631, 0.1121	0.1521, 0.1259
Goodness-of-fit (GOF)	1.037	1.002
Residual density (e Å^{-3})	−0.287 and 0.544	−0.473 and 0.453

Microanalytical data (C, H, N) were collected from a Perkin-Elmer 2400 CHNS/O elemental analyzer. Spectroscopic data were obtained using the following instruments: UV–Vis spectra, Perkin Elmer; model Lambda 25; IR spectra (KBr disk, 4000–400 cm^{-1}), Perkin Elmer; model spectrum RX-1; ^{1}H NMR spectra, Bruker (AC) 300 MHz FTNMR spectrometer. ESI mass spectra were recorded on a Micromass Q-ToF mass spectrometer. Molar conductance was measured using a Systronics conductivity meter (Model 304) using ca. 10^{-3} M solutions in acetonitrile. Magnetic susceptibilities were measured on a Gouy balance using $Hg[Co(SCN)_4]$ as the calibrant. Diamagnetic corrections were made using Pascal's constants.

2.2. Synthesis of the ligand (*HL*)

2-((Pyridine-2-yl)methylthio)benzenamine (3.46 g, 16 mmol) was dissolved in 20 mL of ca.6 M hydrochloric acid and diazotized by adding 10 mL sodium nitrite (1.10 g, 16 mmol) solution at a

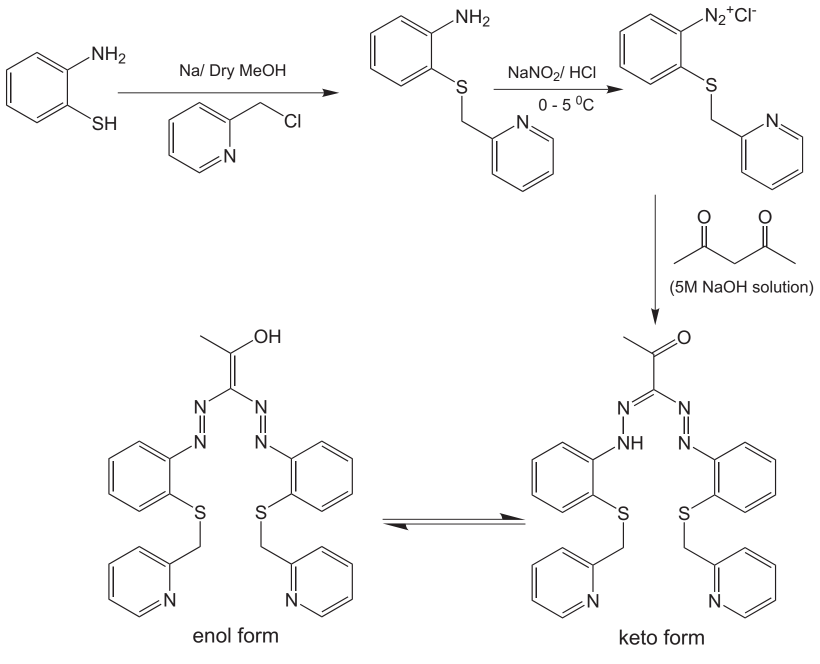

Scheme 1. Synthetic route of ligand **HL**.

Table 2
Some selected X-ray and calculated (DFT/B3LYP method) bond distances (Å) and angles (°) for **1** and **2**.

	M = Ni (**1**)		M = Cu (**2**)	
	X-ray	Calc.	X-ray	Calc.
Bonds (Å)				
M(1)–N(1)	2.122(3)	2.193	2.427(4)	2.402
M(1)–N(2)	1.998(3)	2.040	1.957(3)	2.011
M(1)–N(5)	1.994(3)	2.033	1.945(3)	2.002
M(1)–N(6)	2.137(3)	2.188	2.379(4)	2.385
M(1)–S(1)	2.3667(16)	2.412	2.3294(17)	2.382
M(1)–S(2)	2.3595(15)	2.403	2.3368(17)	2.374
N(2)–N(3)	1.293(3)	1.289	1.295(5)	1.298
N(4)–N(5)	1.291(3)	1.287	1.291(5)	1.307
C(13)–N(3)	1.349(5)	1.346	1.355(5)	1.364
C(13)–N(4)	1.352(5)	1.354	1.323(5)	1.359
C(13)–C(14)	1.500(5)	1.510	1.499(6)	1.510
C(14)–O(1)	1.205(5)	1.216	1.214(5)	1.228
Angles (°)				
N(1)–M(1)–N(2)	87.58(10)	88.16	91.28(12)	89.53
N(1)–M(1)–N(5)	96.02(10)	96.77	96.13(12)	97.92
N(1)–M(1)–N(6)	175.12(9)	172.7	168.52(11)	168.0
N(1)–M(1)–S(1)	83.48(8)	82.06	79.57(9)	79.75
N(1)–M(1)–S(2)	94.27(8)	93.43	91.57(9)	92.41
N(2)–M(1)–N(5)	90.44(11)	89.51	91.19(13)	91.39
N(2)–M(1)–N(6)	94.77(10)	96.23	96.40(12)	98.25
N(2)–M(1)–S(1)	86.17(8)	85.11	87.09(9)	86.03
N(2)–M(1)–S(2)	176.58(8)	174.5	176.71(9)	177.0
N(5)–M(1)–N(6)	88.25(10)	89.06	92.24(12)	91.03
N(5)–M(1)–S(1)	176.59(8)	174.5	175.32(10)	176.5
N(5)–M(1)–S(2)	86.51(8)	85.11	86.88(10)	86.10
N(6)–M(1)–S(1)	92.40(8)	92.52	92.28(9)	91.62
N(6)–M(1)–S(2)	83.61(8)	82.71	81.03(9)	80.19
S(1)–M(1)–S(2)	96.89(4)	99.21	95.04(4)	96.52

temperature of 0 °C. The diazotized solution was added under stirring conditions to acetylacetone (0.80 g, 8 mmol) dissolved in 30 mL of 5 M sodium hydroxide solution. A deep red precipitate was formed which was collected by filtration. The residue was dissolved by adding 1(N) HCl and then NaOH solution was added to it for re-precipitation of the compound. It was filtered and washed with distilled water dried over $CaCl_2$. Yield: 3.08 g, 75%.

Microanalytical data for $C_{27}H_{24}N_6OS_2$ (HL). *Anal.* Calc.: C, 63.26; H, 4.72; N, 16.39. Found: C, 63.26; H, 4.71; N, 16.37%. IR (KBr disc, cm^{-1}): 3365–3256 (NH), 2926 ν(CH), 1677 ν(C=O), 1584 ν(C=N), 1438 ν(N=N). ^{1}H NMR ($CDCl_3$, δ, ppm): 14.97 (s, 1H), 8.42 (d, *J* = 4.1 Hz, 1H), 7.87 (d, *J* = 7.9 Hz, 2H), 7.05–7.50 (m, 12H), 4.16 (s, 4H), 2.62 (s, 3H). UV–Vis (acetonitrile, λ_{max}, nm (ε, M^{-1} cm^{-1})): 460 (18392), 304 (17220), 265 (29260).

2.3. Synthesis of the complexes

To a 15 mL methanolic solution of HL (0.15 g, 0.29 mmol), a $Ni(ClO_4)_2{\cdot}6H_2O$ solution (0.11 g, 0.30 mmol) was added dropwise under stirring conditions. The stirring was further continued for 4 h. The resultant deep pink solution was kept for slow evaporation of the solvent. After a week, a pink crystal suitable for a single crystal X-ray diffraction study of **1** was found. Yield: 0.14 g, 73%.

Microanalytical data for $C_{27}H_{23}ClN_6NiO_5S_2$ (**1**). *Anal.* Calc.: C, 48.42; H, 3.46; N, 12.55. Found: C, 48.52; H, 3.47; N, 12.58%. IR (KBr disc, cm^{-1}): 1666 ν(C=O), 1601 ν(C=N), 1356 ν(N=N), 1093 $\nu(ClO_4^-)$. UV–Vis (acetonitrile, λ_{max}, nm (ε, M^{-1} cm^{-1})): 563 (8420), 528 (8162), 497 (5438), 427 (2628), 317 (7225), 263 (14967). Molar conductance (acetonitrile, λ_M, Ω^{-1} mol^{-1} cm^2): 128. μ_{eff} (B.M.): 3.03.

Complex **2** was prepared following the same procedure as described above by the reaction of $Cu(ClO_4)_2{\cdot}6H_2O$ (0.10 g, 0.28 mmol) with HL (0.11 g, 0.30 mmol) and the resultant pink solution was kept for slow evaporation to grow single crystals suitable for an X-ray diffraction study. Yield: 0.13 g, 68%.

Microanalytical data for $C_{27}H_{23}ClCuN_6O_5S_2$ (**2**). *Anal.* Calc.: C, 48.07; H, 3.44; N, 12.46. Found: C, 48.14; H, 3.46; N, 12.49%. IR data (KBr disc, cm^{-1}): 1658 ν(C=O), 1602 ν(C=N), 1353 ν(N=N), 1118 and 1086 $\nu(ClO_4^-)$. UV–Vis (acetonitrile, λ_{max}, nm (ε, M^{-1} cm^{-1})): 557 (9443), 521 (9013), 490 (5868), 412 (12329), 293 (23645), 263 (26473). Molar conductance (acetonitrile, Λ_M, Ω^{-1} mol^{-1}-cm^2): 135. μ_{eff} (B.M.): 1.97.

2.4. Crystal data collection and refinement

Single crystals suitable for X-ray diffraction of **1** and **2** were grown by slow evaporation of the reaction mixture in methanol over a week. Details of the crystal analysis, data collection and structure refinement data are given in Table 1. Data were collected using a Bruker AXS Kappa Apex-II diffractometer equipped with an Apex-II CCD area detector using a graphite monochromator, Mo Kα radiation (0.71073 Å). Reflection data were recorded using the ω scan technique. For complex **1**, out of 19 751 collected data, 4859

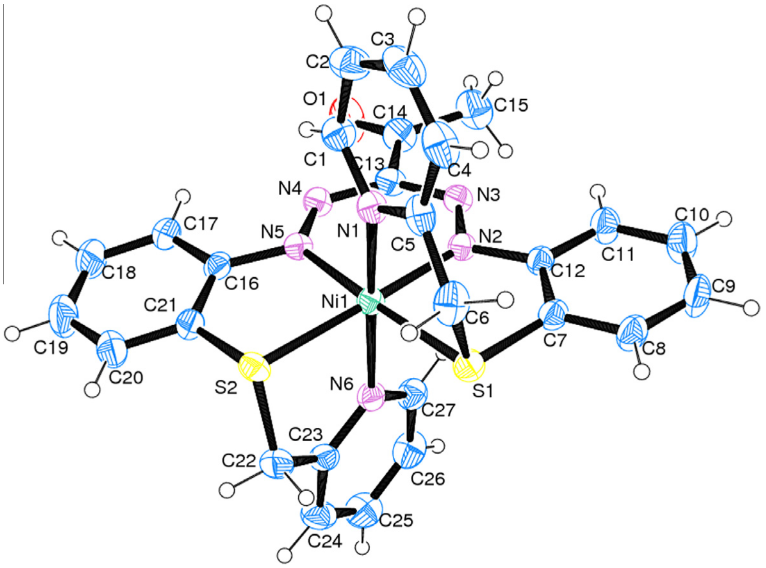

Fig. 1. ORTEP plot of **1** with 35% ellipsoidal probability, with the atom numbering scheme.

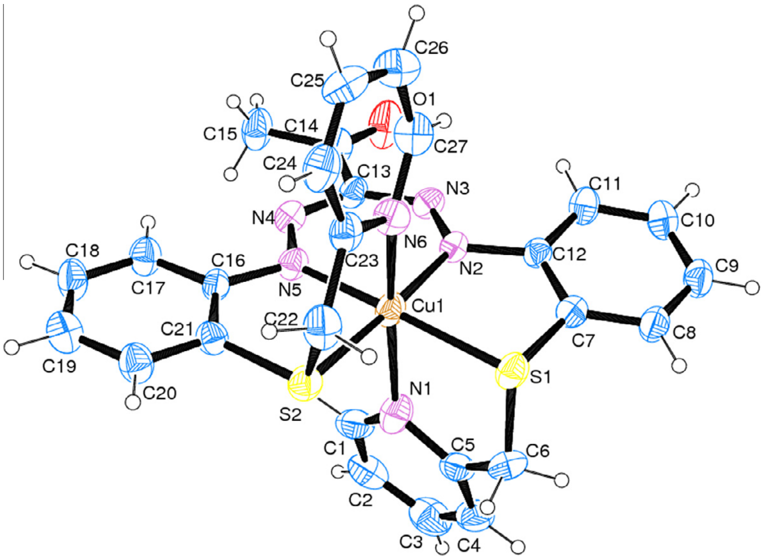

Fig. 2. ORTEP plot of **2** with 35% ellipsoidal probability, with the atom numbering scheme.

with $I > 2\sigma(I)$ within the θ range $1.51 < \theta < 25.08°$ and for **2**, out of 43 413 collected data, 5650 with $I > 2\sigma(I)$ within the θ range $2.03 < \theta < 26.00°$ were used for the structure solution. The data were corrected for Lorentz polarization effects, and absorption corrections were made using SADABS [32]. The structures were solved and refined by full-matrix least-squares techniques on F^2 using the SHELXS-97 program [33]. All non-hydrogen atoms were refined anisotropically. Hydrogen atoms were generated using SHELXL-97 [33], their positions calculated based on the riding model, with thermal parameters equal to 1.2 times that of the associated C atoms, and participated in the calculation of the final R-indices. Molecular structures were drawn with the ORTEP-3 [34] program.

2.5. Computational method

Full geometry optimizations were carried out using the density functional theory (DFT) method at the UB3LYP level for **1** and **2** [35,36]. All elements, except Ni and Cu, were assigned to the 6-31G(d) basis set [37,38]. The LanL2DZ basis set, with an effective core potential for Ni and Cu, was used [39]. The vibrational frequency calculations were performed to ensure that the optimized geometries represent the local minima and that there are only positive eigen values. All calculations were performed with the GAUSSIAN03 program package [40] with the aid of the GaussView visualization program. Vertical electronic excitations based on B3LYP optimized geometries were computed using the time-dependent density functional theory (TDDFT) formalism [41–43] in methanol using a conductor-like polarizable continuum model (CPCM) [44–46]. GaussSum [47] was used to calculate the fractional contributions of various groups to each molecular orbital.

3. Results and discussion

3.1. Synthesis and formulation

The new hexadentate ligand **HL** was synthesized by diazotization of 2-((pyridine-2-yl)methylthio)benzenamine followed by coupling with acetylacetone in NaOH solution (Scheme 1). It was characterized by elemental, mass and spectral analysis. The mass spectrum shows a peak at m/z 513([M−H]$^+$) corresponding to **HL**. ^{1}H NMR analysis in $CDCl_3$ has found a singlet at 14.97 ppm, corresponding to the N–H proton, and a broad stretching at 3260–3375 cm^{-1} along with a sharp peak at 1676 cm^{-1} in the IR spectrum indicates the existence of the keto form of the ligand (see Section 2) (Scheme 1). The ν(C═N) and ν(N═N) bands appeared at 1625 and 1438 cm^{-1} respectively. In the course of the reaction **HL** loses its N–H proton in the presence of Et_3N and the negative charge so formed is stabilized by resonance with the two adjacent azo groups. The keto form of the ligand has been established in the octahedral Ni(II) and Cu(II) complexes, [Ni(L)](ClO_4) (**1**) and [Cu(L)](ClO_4) (**2**). The IR spectra of the complexes show a sharp peak at 1658–1666 cm^{-1}, corresponding to ν(C═O) of the ligand. The ν(N═N) band in the complexes is red shifted and observed at 1353–1356 cm^{-1}. This is due to participation of the N═N bond in resonance with the negative charge and $d\pi$ (M) → π^*(N═N) back donation. The complexes show molar conductance values in the range 128–132 Ω^{-1} mol^{-1} cm^2 in acetonitrile solution, corresponding to a 1:1 electrolyte.

3.2. Molecular structures of 1 and 2

The molecular structures of the complexes were confirmed by single crystal X-ray diffraction studies. The bond parameters show the distorted octahedral geometry around Ni and Cu in the isostructural complexes **1** and **2**, respectively. Selected bond distances and bond angles are given in Table 2. The ORTEP views with the atom numbering schemes are shown in Figs. 1 and 2 for **1** and **2**, respectively. The hexadentate (N,S,N,N,S,N) donor ligand coordinates with central metal ion with two pyridyl-N, two thioether-S and two azo-N atoms. The ligand in the complexes is mono anionic and the negative charge is delocalized between two adjacent azo groups, N(2)–N(3) and N(4)–N(5). Consequently, the azo bond distances (N(2)–N(3), 1.293(3) Å in **1** and 1.295(5) Å in **2**, N(4)–N(5), 1.291(3) Å in **1** and 1.291(5) Å in **2**) are elongated compared to the N═N distances in related reported complexes [48,49] and the C(13)–N(3), 1.349(5) Å in **1**, 1.355(5) Å in **2**, and C(13)–N(4), 1.352(5) Å in **1** and 1.355(5) Å in **2**, bond distances are shorter than the expected C–N single bond distance. The O(1)–C(14) bond (1.205(5) Å in **1** and 1.214(5) Å in **2**) in the complexes perfectly match with C═O (keto) distances and well correlate with the ν(CO) stretching value (1658–1666 cm^{-1}) in the IR studies. The C–C distance (C(13)–C(14), 1.500(5) Å in **1** and 1.499(6) Å in **2**) adjacent to the C═O function has single bond character. The M–N(azo), 1.998(3)/1.994(3) Å in **1** and 1.957(3)/1.945(3) Å in **2**, bonds are much shorter than the M–N(pyridyl), 2.122(3)/2.137(3) Å in **1** and 2.427(4)/2.379(3) Å in **2**, bond distances, which well support the $d\pi$ (M) → π^*(N=N) back donation process and elongation of axial bonds in the complexes. The Cu–N(azo) bonds are ~0.045 Å shorter than the Ni–N(azo) distances, indicating facile $d\pi$ (M) → π^*(N=N) back donation in complex **2** compared to complex **1**. The M–S(thioether) distances (2.3667(16)/2.3595(15) Å in **1** and 2.3294(17)/2.3368(17) Å in **2**) are well matched to reported bond distances [48–51]. Most importantly the X-ray structure metrical parameters show that the Cu–N(azo) and Cu–S(thioether) bond distances in **2** are shorter than the Ni–N(azo) and Ni–S(thioether) distances in **1**, whereas the Cu–N(pyridyl) in **2** bond distances are significantly longer than Ni–N(pyridyl) distances in **1**.

3.3. Electronic structure DFT calculations

The coordinates obtained from single crystal X-ray diffraction data for complexes **1** and **2** were optimized using the DFT/UB3LYP (LANL2DZ/6-31G(d)) level of calculations in triplet (S = 1) and doublet (S = ½) states respectively. The optimized bond parameters well correlate with the X-ray data (Table 2).

For complex **1**, the singly occupied molecular orbitals (SOMOs) are concentrated on the ligand (95%). The other low energy α-spin occupied molecular orbitals are composed of mainly a ligand group of orbitals, with a reduced contribution of $d\pi$ (Ni) orbitals. The β-spin occupied orbitals are also concentrated on the ligand, with a minor contribution (12%) of $d\pi$ (Ni) in HOMO−2. The α-spin unoccupied MOs and the β-spin LUMO has ligand character, but LUMO+1 and LUMO+2 of β-spin have 62% and 75% metal $d_{x^2-y^2}$ and d_{z^2} character, with a reduced contribution from the ligand (Table S1, Fig. S2). Similarly, the SOMO and other α-spin occupied and unoccupied molecular orbitals for **2** are composed of a ligand group of orbitals with a minor contribution (25%) of the $d\pi$ (Cu) orbital in HOMO−3. The β-spin occupied orbials have ligand character, with a $d\pi$ (Cu) contribution in HOMO−2 and HOMO−3. The β-spin LUMO has $d\pi$ (Cu) character and other low energy unoccupied orbitals have π^*(L) character (Table S2, Fig. S3).

3.4. Spectral properties and TDDFT calculations

To simulate the experimental electronic spectra, TDDFT/B3LYP/CPCM calculations for **HL**, **1** and **2** have been performed in methanol. The calculated vertical electronic transitions calculated by the TDDFT method are given in Tables 3–5 for **HL**, **1** and **3** respectively.

The ligand in methanol shows peaks at 460, 304, 265 and 203 nm. The low energy band corresponds to a mixture of $n \to \pi^*$

Table 3
Vertical electronic excitations calculated by the TD DFT/B3LYP/CPCM method and experimental absorption bands of **HL**.

$E_{\text{excitation}}$ (eV)	$\lambda_{\text{excitation}}$ (nm)	Osc. strength f	Key transitions	Character	$\lambda_{\text{expt.}}$ (ε, M^{-1} cm^{-1})
2.4245	511	0.02	(67%) HOMO → LUMO+1	$n \to \pi^*$	460 (18392)
2.8139	441	0.17	(59%) HOMO–1 → LUMO (21%) HOMO → LUMO+1	$n/\pi \to \pi^*$	
3.8413	323	0.14	(74%) HOMO–3 → LUMO+1	$\pi \to \pi^*$	304 (17220)
3.8946	318	0.09	(40%) HOMO–4 → LUMO (23%) HOMO–8 → LUMO	$\pi \to \pi^*$	
4.2143	294	0.09	(56%) HOMO → LUMO+3 (24%) HOMO → LUMO+2	$n \to \pi^*$	
4.3214	287	0.09	(64%) HOMO–5 → LUMO	$\pi \to \pi^*$	265 (29260)
4.3749	283	0.08	(65%) HOMO–1 → LUMO+2	$\pi \to \pi^*$	

Table 4
Vertical electronic excitations calculated by the TD DFT/UB3LYP/CPCM method and experimental absorption bands of **1**.

$E_{\text{excitation}}$ (eV)	$\lambda_{\text{excitation}}$ (nm)	Osc. strength f	Key transition	Character	$\lambda_{\text{expt.}}$ (ε, M^{-1} cm^{-1})
2.1940	565	0.05	(72%) HOMO–1(β) → LUMO(β)	ILCT	563 (8420)
2.4597	504	0.05	(87%) HOMO–2(α) → LUMO(α)	ILCT	528 (8162)
2.6082	475	0.22	(35%) HOMO(β) → LUMO(β) (32%) HOMO–2(β) → LUMO(β)	ILCT ILCT, MLCT	497 (5438)
2.6653	465	0.17	(37%) HOMO–2(β) → LUMO(β) (23%) HOMO(β) → LUMO(β)	ILCT, MLCT ILCT	
3.8552	322	0.27	(81%) HOMO–1(α) → LUMO+2(α)	ILCT	317 (sh)
4.1717	297	0.09	(47%) HOMO–3(β) → LUMO+3(β) (25%) HOMO–4(β) → LUMO+3(β)	ILCT	
4.5465	273	0.31	(72%) HOMO–5(β) → LUMO+3(β)	ILCT	263 (14967)

Table 5
Vertical electronic excitations calculated by the TD DFT/UB3LYP/CPCM method and experimental absorption bands of **2**.

$E_{\text{excitation}}$ (eV)	$\lambda_{\text{excitation}}$ (nm)	Osc. strength f	Key transition	Character	$\lambda_{\text{expt.}}$ (ε, M^{-1} cm^{-1})
2.1589	574	0.06	(94%) HOMO–1(β) → LUMO(β)	LMCT, ILCT	557 (9443)
2.3932	518	0.08	(77%) HOMO–2(β) → LUMO(β)	LMCT, ILCT	521 (9013)
2.4078	515	0.07	(41%) HOMO(β) → LUMO+1(β) (31%) HOMO–8(β) → LUMO(β)	LMCT, ILCT	490 (5868)
2.5407	488	0.03	(65%) HOMO–3(β) → LUMO(β)	LMCT, ILCT	
3.01292	411	0.04	(88%) HOMO–4(β) → LUMO+1(β)	ILCT	412 (12329)
3.4027	364	0.25	(42%) HOMO–6(β) → LUMO+1(β) (27%) HOMO–8(β) → LUMO+1(β)	ILCT	
3.9969	310	0.13	(67%) HOMO–4(β) → LUMO+1(β)	ILCT	293 (sh)
4.1929	296	0.22	(78%) HOMO–5(β) → LUMO+1(β)	ILCT	
4.6769	265	0.37	(36%) HOMO–7(β) → LUMO+1(β) (33%) HOMO–8(β) → LUMO+1(β)	ILCT	263 (26473)

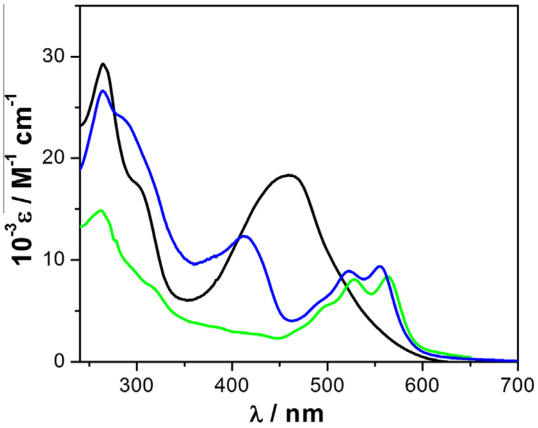

Fig. 3. UV–Vis spectra of **HL** (——), **1** (——) and **2** (——) in acetonitrile.

and $\pi \rightarrow \pi^*$ character, while the high energy bands are due to $\pi \rightarrow \pi^*$ transitions (Table 3). In complex **1**, three closely spaced, moderately intense bands at 563, 528 and 497 nm have been observed, along with a sharp intense band at 263 nm and two weak peaks at 427 and 317 nm (Fig. 3). The TDDFT calculation shows that the low energy closely spaced peaks are due to intra-ligand charge transfer transitions with partial mixing of $d\pi$ (Ni) → π (L), MLCT transitions. The high energy bands correspond to intra-ligand charge transfer (ILCT) transitions (Table 4). For complex **2**, low energy bands are observed at 557, 521 and 490 nm. The ligand centered transitions are observed at 412, 293 and 263 nm. The calculated transitions at 574 and 518 nm have mixed ILCT, MLCT and LMCT character, along with a minor contribution of *d*–*d* transitions (Table 5). The other transitions at 515, 488, 411 and 365 nm correspond to mixed LMCT and ILCT character.

3.5. Magnetic moment measurements

The magnetic moment measurements in the solid state show that the present complexes are paramagnetic at room temperature. The observed magnetic moments of these complexes are 3.03 and 1.97 B.M. for **1** and **2** respectively. These values are quite close to the values expected for spin free octahedral nickel(II) and copper(II) complexes [52,53], and are characteristic of d^8 and d^9 electronic configurations of Ni(II) and Cu(II) in **1** and **2** respectively.

4. Conclusion

The new thioether containing a hexadentate azo-ligand (**HL**), having pyridyl-N, thioether-S and azo-N donor atoms, has been synthesized and characterized. The octahedral complexes of Ni(II) and Cu(II) were synthesized and characterized. The structures of the complexes have been confirmed by single crystal X-ray diffraction. In the complexes the ligand loses one proton and acts as a carbanion. The carbanion is stabilized by delocalization with the adjacent two azo functions. The electronic structures and spectral properties of the ligand and the complexes have been explained by DFT and TD DFT calculations.

Acknowledgements

Financial support received from the Department of Science and Technology, New Delhi, India is gratefully acknowledged. M.S. Jana and A.K. Pramanik are thankful to CSIR, New Delhi, India for fellowships.

Appendix A. Supplementary data

CCDC 821874 and 810470 contains the supplementary crystallographic data for **1** and **2**. These data can be obtained free of charge via http://www.ccdc.cam.ac.uk/conts/retrieving.html, or from the Cambridge Crystallographic Data Centre, 12 Union Road, Cambridge CB2 1EZ, UK; fax: (+44) 1223-336-033; or e-mail: deposit@ccdc.cam.ac.uk. Supplementary data associated with this article can be found, in the online version, at http://dx.doi.org/10.1016/j.poly.2014.03.052.

References

[1] R.A. Allred, S.A. Hufner, K. Rudzka, A.M. Arif, L.M. Berreau, Dalton Trans. (2007) 351.
[2] M.R. Malachonsk, M. Adams, N. Elia, A.L. Rheingold, R.S. Kelly, J. Chem. Soc., Dalton Trans. (1999) 2177.
[3] B. Adhikary, S. Liu, C.R. Lucas, Inorg. Chem. 32 (1993) 5957.
[4] K. Pramanik, S. Karmakar, S.B. Choudhury, A. Chakravorty, Inorg. Chem. 36 (1997) 3562.
[5] S. Mukhopadhyay, D. Ray, J. Chem. Soc., Dalton Trans. (1995) 265.
[6] S. Karmakar, S.B. Choudhury, D. Ray, A. Chakravorty, Polyhedron 12 (1993) 2325.
[7] A.K. Singh, R. Mukherjee, Dalton Trans. (2005) 2886.
[8] C. Belle, W. Rammal, J.-L. Pierre, J. Inorg. Biochem. 99 (2005) 1929.
[9] R. Lill, Nature 460 (2009) 831.
[10] F. Thomas, Eur. J. Inorg. Chem. (2007) 2379.
[11] L. Zhou, D. Powell, K.M. Nicholas, Inorg. Chem. 46 (2007) 7789.
[12] M. Rombach, J. Seebacher, M. Ji, G. Zhang, G. He, M.M. Ibrahim, B. Benkmil, H. Vahrenkamp, Inorg. Chem. 45 (2006) 4571.
[13] L.M. Berreau, Eur. J. Inorg. Chem. (2006) 273.
[14] R.L. Richard, Coord. Chem. Rev. 154 (1996) 83.
[15] R.P. Happe, W. Roseboom, A.J. Pierik, S.P. Albracht, K.A. Bagley, Nature 385 (1997) 126.
[16] A. Volveda, E. Gracin, C. Piras, A.L. Delacey, V.M. Fernandez, E.C. Hatchikian, M. Frey, J.C. Fontecilla-Camps, J. Am. Chem. Soc. 118 (1996) 12989.
[17] A. Volveda, M.H. Charon, C. Piras, E.C. Hatchikian, M. Frey, J.C. Fontecilla-Camps, Nature 373 (1995) 580.
[18] R. Cammack, Nature 373 (1995) 556.
[19] R.M. Buonomo, I. Font, M.J. Maguire, J.H. Reibenspies, T. Tuntulani, M.Y. Darensbourg, J. Am. Chem. Soc. 117 (1995) 963.
[20] R.H. Holm, P. Kennepohl, E.I. Solomon, Chem. Rev. 96 (1996) 2239.
[21] E.I. Solomon, P.E. Palmer, Angew. Chem., Int. Ed. 40 (2001) 4570.
[22] W. Kaim, J. Rall, Angew. Chem. 108 (1996) 47.
[23] K.S. Banu, T. Chattopadhyay, A. Banerjee, S. Bhattacharaya, E. Suresh, M. Nethaji, E. Zangrando, D. Das, Inorg. Chem. 47 (2008) 7083.
[24] T. Chattopadhyay, M. Mukherjee, A. Mondal, P. Maiti, A. Banerjee, K.S. Banu, S. Bhattacharya, B. Roy, D.J. Chattopadhyay, T.K. Mondal, M. Nethaji, E. Zangrando, D. Das, Inorg. Chem. 49 (2010) 3121.
[25] R. Cammack, in: J.R. Lancaster Jr. (Ed.), The Bioinorganic Chemistry of Nickel, VCH, New York, 1988. Chap. 8.
[26] S.W. Ragsdale, H.G. Wood, J.A. Marton, L.G. Ljungdahl, D.V. DerVartanian, in: J.R. Lancaster Jr. (Ed.), The Bioinorganic Chemistry of Nickel, VCH, New York, 1988. Chap. 14.
[27] S.B. Choudhury, D. Roy, A. Chakravorty, Inorg. Chem. 29 (1990) 4603.
[28] D.R. Matazo, R.A. Ando, A.C. Borin, P.S. Santos, J. Phys. Chem. A 112 (2008) 4437.
[29] T. Hihara, Y. Okada, Z. Morita, Dyes Pigments 59 (2003) 25.
[30] K.H. Saunders, R.L.M. Allen, Aromatic Diazo Compounds, third ed., Edward Arnold, London, 1985.
[31] P. Chattopadhyay, Y.H. Chiu, J.M. Lo, C.S. Chung, T.H. Lu, Appl. Radiat. Isot. 52 (2000) 217.
[32] G.M. Sheldrick, Program for Empirical Absorption Correction, University of Göttingen, Göttingen, Germany, 1996.
[33] G.M. Sheldrick, SHELX97, Programs for Crystal Structure Analysis; University of Göttingen, Göttingen, Germany, 1997.
[34] L.J. Farrugia, J. Appl. Crystallogr. 30 (1997) 565.
[35] A.D. Becke, J. Chem. Phys. 98 (1993) 5648.
[36] C. Lee, W. Yang, R.G. Parr, Phys. Rev. B 37 (1988) 785.
[37] G.A. Petersson, A. Bennett, T.G. Tensfeldt, M.A. Al-Laham, W.A. Shirley, J. Mantzaris, J. Chem. Phys. 89 (1988) 2193.
[38] G.A. Petersson, M.A. Al-Laham, J. Chem. Phys. 94 (1991) 6081.
[39] P.J. Hay, W.R. Wadt, J. Chem. Phys. 82 (1985) 299.
[40] M.J. Frisch, G.W. Trucks, H.B. Schlegel, G.E. Scuseria, M.A. Robb, J.R. Cheeseman, J.A. Montgomery Jr., T. Vreven, K.N. Kudin, J.C. Burant, J.M. Millam, S.S. Iyengar, J. Tomasi, V. Barone, B. Mennucci, M. Cossi, G. Scalmani, N. Rega, G.A. Petersson, H. Nakatsuji, M. Hada, M. Ehara, K. Toyota, R. Fukuda, J. Hasegawa, M. Ishida, T. Nakajima, Y. Honda, O. Kitao, H. Nakai, M. Klene, X. Li, J.E. Knox, H.P. Hratchian, J.B. Cross, V. Bakken, C. Adamo, J. Jaramillo, R. Gomperts, R.E. Stratmann, O. Yazyev, A.J. Austin, R. Cammi, C. Pomelli, J.W. Ochterski, P.Y. Ayala, K. Morokuma, G.A. Voth, P. Salvador, J.J. Dannenberg, V.G. Zakrzewski, S. Dapprich, A.D. Daniels, M.C. Strain, O. Farkas, D.K. Malick, A.D. Rabuck, K.

Raghavachari, J.B. Foresman, J.V. Ortiz, Q. Cui, A.G. Baboul, S. Clifford, J. Cioslowski, B.B. Stefanov, G. Liu, A. Liashenko, P. Piskorz, I. Komaromi, R.L. Martin, D.J. Fox, T. Keith, M.A. Al-Laham, C.Y. Peng, A. Nanayakkara, M. Challacombe, P.M.W. Gill, B. Johnson, W. Chen, M.W. Wong, C. Gonzalez, J.A. Pople, GAUSSIAN 03, Revision D.01, GAUSSIAN Inc., Wallingford CT (2004).
[41] R. Bauernschmitt, R. Ahlrichs, Chem. Phys. Lett. 256 (1996) 454.
[42] R.E. Stratmann, G.E. Scuseria, M.J. Frisch, J. Chem. Phys. 109 (1998) 8218.
[43] M.E. Casida, C. Jamorski, K.C. Casida, D.R. Salahub, J. Chem. Phys. 108 (1998) 4439.
[44] V. Barone, M. Cossi, J. Phys. Chem. A 102 (1998) 1995.
[45] M. Cossi, V. Barone, J. Chem. Phys. 115 (2001) 4708.
[46] M. Cossi, N. Rega, G. Scalmani, V. Barone, J. Comput. Chem. 24 (2003) 669.
[47] N.M. O'Boyle, A.L. Tenderholt, K.M. Langner, J. Comput. Chem. 29 (2008) 839.
[48] P.K. Dhara, S. Pramanik, T.-H. Lu, M.G.B. Drew, P. Chattopadhyay, Polyhedron 23 (2004) 2457.
[49] D. Banerjee, U.S. Ray, S.K. Jasimuddin, J.-C. Liou, T.-H. Lu, C. Sinha, Polyhedron 25 (2006) 1299.
[50] P.K. Dhara, S. Sarkar, M.G.B. Drew, M. Nethaji, P. Chattopadhyay, Polyhedron 27 (2008) 2447.
[51] S. Nandi, D. Bannerjee, J.S. Wu, T.H. Lu, A.M.Z. Slawin, J.D. Woollins, J. Ribas, C. Sinha, Eur. J. Inorg. Chem. (2009) 3972.
[52] R.N. Patel, N. Singh, V.L.N. Gundla, Polyhedron 26 (2007) 757.
[53] P.A.N. Reddy, B.K. Santra, M. Nethaji, A.R. Chakravarty, J. Inorg. Biochem. 98 (2004) 377.